MINISTRY OF EDUCATION AND TRAINING

VIETNAM ACADEMY OF SCIENCE AND TECHNOLOGY

GRADUATE UNIVERSITY OF SCIENCE AND TECHNOLOGY

Kieu Xuan Hau

INVESTIGATION OF THE STRUCTURE AND PROPERTIES OF Ni-Ti AND Ni-Mn BASED SHAPE MEMORY ALLOYS PREPARED BY RAPIDLY QUENCHED METHOD

SUMMARY OF DISSERTATION ON SCIENCE OF MATTER

Major: Electronic materials

Code: 9 44 01 23

Ha Noi - 2025

The dissertation is completed at: Graduate University of Science and Technology, Vietnam Academy Science and Technology

Supervisors:

1. Supervisor 1: GS.TS. Nguyen Huy Dan, Institute of Materials Science, Vietnam Academy of Science and Technology

2. Supervisor 2: TS. Nguyen Hai Yen, Institute of Materials Science - Vietnam Academy of Science and Technology

Referee 1: PGS.TS. Luu Tien Hung

Referee 2: PGS.TS. Nguyen Cao Khang

Referee 3: PGS.TS. Nguyen Hoang Nam

The dissertation is examined by Examination Board of Graduate University of Science and Technology, Vietnam Academy of Science and Technology at 9:00 a.m., May 13, 2025.

The dissertation can be found at:

1. Graduate University of Science and Technology Library

2. National Library of Vietnam

INTRODUCTION

Shape Memory Alloys (SMAs) have attracted the attention of researchers due to their unique properties and diverse application potential. SMAs are a group of materials that have the ability to return to their original shape under the influence of temperature or magnetic field. It is well known that the SMAs undergo a structural transformation from high temperature austenitic phase to low temperature martensitic one. Because of the unique features of the Ni-Ti alloys, they have been widely used in various fields of industry, aerospace and biomedicine, such as couplings, actuators, orthodontic arches, and stents. The Shape Memory Effect (SME) in alloys was first discovered in 1932 by Ölander on Au-Cd alloys. Later, many other SMAs were fabricated such as Cu-based alloys (Cu-Zn, Cu-Sn), Ni-based alloys (Ni-Ti, Ni-Mn), Fe-based alloys (Fe-Pd, Fe-Pt)...

Among SMAs, Ni-Ti alloys are the most widely used because they not only possess a good SME, mechanical and corrosion resistance but also have high biological compatibility. Therefore, they have been widely used in industrial and biomedical fields. Although widely used in the past few decades, Ni-Ti alloys have shown some disadvantages that prevent the expansion of their applications in practice. These are bad deformation at low temperatures, high material cost, slow reaction to temperature change, small operating temperature range and poor repeatability. Therefore, some researchers have added other elements (Cu, Fe, Zr, Hf...) into Ni-Ti alloys and changed the manufacturing technology conditions to minimize the disadvantages of these alloys. The addition of Cu to the binary Ni-Ti SMAs reduces the transformation temperature hysteresis, enhances the shape memory properties and improves the mechanical properties. By adding more elements (more than 3 elements), the alloy can form a high entropy shape memory alloy (HESMA). The combination of preeminent features of shape memory and high entropy alloys (high durability, heat resistance, low diffusion coefficient) will provide potential applications in practice.

For SMAs that are affected by an external magnetic field, also known as Magnetic shape memory alloys (MSMA), their SME is stimulated not only by temperature but also by magnetic field. With magnetic stimulation, the response time of the SME is very fast and more accurate than in the case of temperature stimulation. Besides, the lifetime is longer and the ability to create deformation and stress is also much greater than those of magnetostrictive or piezoelectric materials. Normally, MSME occurs in materials possessing a magnetic transition from a paramagnetic or weak ferromagnetic phase to a ferromagnetic one. These magnetic phase transitions undergo a structural change or a first-order phase transition. In Ni-Mn-based Heusler alloys (Ni-Mn-Ga, Ni-Mn-Sn, Ni-Mn-Sb, Ni-Mn-Al...), MSME occurs through M-A structural transformations and magnetic interactions in the material. Large magnetic field-induced deformation was first observed in Ni-Mn-based Heusler MSMA (Ni_2MnGa) in 1996. Later, many Heusler MSMAs besides Ni_2MnGa were reported such as Ni-Mn-Z (Z = In, Sn, Sb, Al). These MSMAs have different advantages and disadvantages. Ni-Mn-Ga alloys have large strain (up to 10%) caused by external magnetic fields. However, this alloy is brittle, high cost so it is rarely used in practice. Ni-Mn-Al alloy has a structural transformation temperature close to room temperature, good mechanical properties and relatively low cost. However, the temperature hysteresis of Ni-Mn-Al alloy is large. Recently, it has been reported that Co-doped Ni-Mn-(Ga,Al) alloys show a drastic change in the magnetic phase transition. The substitution of Ni by Co affects the magnetic exchange interactions and the ferromagnetic phases of the alloys leading to an enhancement of the magnetic field-induced martensitic-austenitic transformation for the alloys. The structure and magnetic properties of alloys are significantly affected by the fabrication technology. Previous studies mainly focused on bulk samples. For Ni-Mn based MSMAs, bulk alloy samples require an annealing process with high temperature and a long time (for several days). However, alloy ribbons prepared by the rapidly quenched method can have the desired structure and

properties without annealing. In addition, the shape of the alloy ribbons is suitable for their use in some practical applications such as actuators or sensors.

In Viet Nam, there have been some remarkable research results on shape memory alloy such as the International Training Institute for Materials Science (ITIMS) - Hanoi University of Science and Technology, School of Materials Science and Engineering - Hanoi University of Science and Technology, Faculty of Engineering Mechanics and Automation, University of Engineering and Technology - Vietnam National University, Hanoi and Institute of Materials Science - Vietnam Academy of Science and Technology. However, the research results, both fundamental and applied, have not been widely published. Therefore, studying the structure and properties of shape memory alloys to be able to apply them to different applications in practice is still an issue that needs attention.

To achieve the above purpose, the research topic of the thesis was selected as ***"Investigation of the structure and properties of Ni-Ti and Ni-Mn based shape memory alloys prepared by rapidly quenched method".***

The research objectives of the thesis:

- Ni-Ti based shape memory alloys: (Ni,Cu)-Ti, Ni-Cu-Ti-Zr-(Hf,Nb,Co,Cr,Ga).

- Ni-Mn based shape memory alloys: (Ni,Co)-Mn-(Ga,Al).

The goal of the thesis:

Fabrication of Ni-Ti and Ni-Mn shape memory alloys with structures and properties meeting the requirements for applications in biomedicine, micromechanics, aerospace, sensors and automation.

Research contents of the thesis include:

- Fabrication of (Ni,Cu)-Ti, Ni-Cu-Ti-Zr-(Hf,Nb,Co,Cr,Ga), (Ni,Co)-Mn-(Ga,Al) shape memory alloys by rapidly quenched method.

- Investigation of structure and properties of fabricated shape memory alloy.

- Finding out the rule of influence of composition on structure and properties of alloys.

Research Methods:

The thesis was carried out by experimental research methods. The samples were prepared by using melt-spinning methods. The structure, chemical composition and magnetic properties were analyzed by X-ray diffraction (XRD), scanning electron microscopy (SEM), energy dispersive X-ray spectroscopy (EDX), differential thermal analysis (DTA), differential scanning calorimetry (DSC), thermomagnetization M(T) and magnetic hysteresis M(H). The mechanical properties were examined by hardness and tensile stress-strain. The corrosion resistance was studied by electrochemical corrosion measurement.

Scientific meanings of the thesis:

The research results not only contribute to clarifying the SME mechanism in SMAs but also promote the development of smart material technology, serving the increasing needs in industry and life. Clarifying the influence of additional elements on the structure and properties of Ni-Ti and Ni-Mn shape memory alloys will contribute new information to the research on this type of material.

The layout of the thesis:

The thesis consists of 137 pages with 31 tables and 106 figures. In addition to the introduction, conclusion and references, the thesis is presented in 4 chapters as follows:

Chapter 1. Overview of Ni-Ti and Ni-Mn based shape memory alloys.

Chapter 2. Experimental techniques.

Chapter 3. Structure and properties of Ni-Ti-based shape memory alloys.

Chapter 4. Structure and properties of Ni-Mn based shape memory alloys**.**

Main results of the thesis:

- Successfully fabricated Ni-Ti and Ni-Mn-based rapidly quenched shape memory alloys.

- Investigated the structure and properties of the manufactured alloys.

- Observed the martensitic-austenitic (M-A) structural transformation related to the shape memory effect in most of the obtained samples.

- With the Ni-Ti-based SMA, the structural transformation temperature, tensile strength, tensile strain and corrosion resistance enhance by the addition of Cu, Zr, Hf, Co, Nb, Cr and Ga elements. The achieved highest tensile strength and tensile strain were 180 MPa and 2.3% on the Ni-Ti-Cu ternary alloy, respectively. With the Ni-Cu-Ti-Zr-(Hf,Nb,Co,Cr,Ga) HESMA, the M-A structural transformation temperature reach over 500ºC. The achieved highest tensile strength and tensile strain were 669 MPa, 0.9% on the alloy containing Hf. The obtained lowest corrosion rate on the sample containing Ga was 0.09 x 10^{-2} mm/year.

- With the Ni-Mn-based MSMA, the M-A structural transformation temperature of the (Ni,Co)-Mn-Ga alloys can be adjusted in the temperature range from 180 to 360ºC while the M-A structural transformation temperature of the Ni-Co-Mn-Al alloy can be adjusted from 150 to 430ºC. The external magnetic field strongly affects on the M-A structural transformation and the magnetic phase transition of the alloy.

The experimental work of this thesis was mainly carried out on equipment located at the Institute of Materials Science, Vietnam Academy of Science and Technology. Part of the work was carried out at the Institute of Chemistry, Institute of Tropical Technology - Vietnam Academy of Science and Technology and School of Materials Science and Engineering - Hanoi University of Science and Technology, VNU University of Science - Vietnam National University, Hanoi

CHAPTER 1. OVERVIEW OF Ni-Ti AND Ni-Mn BASED SHAPE MEMORY ALLOYS

1.1. Basic concepts and properties of shape memory alloys

Shape memory alloys (SMAs) are materials that have the ability to return to their original shape when subjected to temperature or magnetic field. SMAs can exist in two different crystal structure phases: martensite (stable at low temperatures) and austenite (stable at higher temperatures).

Alloys that have the ability to return to their original shape when subjected to a magnetic field are called magnetic shape memory alloys (MSMA). The advantage of these alloys is that when stimulated by a magnetic field, the response time of the shape memory effect is very fast and more accurate than when stimulated by temperature.

There are four characteristic temperatures associated with the M-A structural transformation in SMAs: the martensitic start temperature (T_s^M), the martensitic finish temperature (T_f^M), the austenitic start temperature (T_s^A) and the austenitic finish temperature (T_f^A).

The structural transformation temperatures can be measured directly by various methods such as differential scanning calorimetry (DSC), and resistivity versus temperature. For MSMAs, these structural transformation temperatures can be determined by M(T) thermomagnetization curves.

In terms of mechanical properties, SMA has some characteristic quantities such as recovery strain (ε_r), strength (σ), and hardness (HV). Recovery strain is very important for SMAs because it determines the ability of the material to return to its original shape after being deformed. In addition to the above quantities, corrosion rate (CR) is also very important for alloys.

1.2. Methods of manufacturing shape memory alloys

Some common methods for manufacturing shape memory alloys include: Melt metallurgy, powder metallurgy, melt-spinning method, sputtering, etc. Depending on the research and application purposes, the appropriate manufacturing method is selected.

1.3. Development and application of shape memory alloys

In 1932, Ölande, a Swedish physicist, discovered SME in Au-Cd alloy.

In 1963, Buehler and Wang discovered SME in Ni-Ti alloy.

In 1996, Heusler Cu-Al-Mn based SMA with relatively high Mn content was published.

In 2014, Firstov studied SME on Ti-Zr-Hf-Ni-Co-Cu HEA. Nowadays, with a better understanding of the properties and application requirements of shape memory materials, research on SMAs has increased significantly.

1.4. Ni-Ti based shape memory alloy

By changing the proportion of Ni or Ti or adding Cu, Zr, Hf, Fe... elements to the alloy with appropriate concentration, the transformation temperature can be adjusted, improving the mechanical properties and the corrosion resistance of the alloy.

1.5. Ni-Mn based shape memory alloy

Ni-Mn-based Heusler MSMA such as Ni-Mn-Z (Z = Ga, Sn, In, Al...) has a coexistence of magnetic phase transition and structural transformation. By changing the composition, the structure, magnetic and mechanical properties of the alloy can be adjusted.

1.6. Some research results on shape memory materials in Vietnam

In Vietnam, there are a number of research groups on shape memory materials, typically: International Training Institute for Materials Science (ITIMS) - Hanoi University of Science and Technology, School of Materials Science and Engineering - Hanoi University of Science and Technology, Faculty of Engineering Mechanics and Automation, University of Engineering and Technology - Vietnam National University, Hanoi and Institute of Materials Science-Vietnam Academy of Science and Technology. The published results as well as the practical application of SMAs in the country are not many.

CHAPTER 2. EXPERIMENTAL TECHNIQUES

2.1. Fabrication of shape memory alloys by using melt-spinning method

Ni-Ti based alloys: $Ni_{50-x}Ti_{50-x}Cu_x$ (x = 0 - 20), $Ni_{25}Cu_{25}Ti_{16,667}Zr_{16,667}A_{16,667}$ (A = Hf, Nb, Co, Cr và Ga) and Ni-Mn based alloys: $Ni_{50}Mn_{50-x}Ga_x$ (*x* = 17 - 21), $Ni_{50-x}Co_xMn_{29}Ga_{21}$ (x = 0 - 8), $Ni_{50-x}Co_xMn_{50-y}Al_y$ (x = 5 - 13 and Al = 15 - 19) were prepared from elements with purity above 99.9%. The arc-melting method was used to prepare the precursors. Then, the alloy ribbons were prepared by the melt-spinning method.

2.2. Methods for studying structure and properties

The structure and chemical composition of the samples were studied by XRD, SEM and EDX. The structural transition temperatures of the alloy

samples were determined by DTA and DSC. The magnetic properties were investigated by M(H) and M(T). The mechanical properties and corrosion resistance were demonstrated by Vickers hardness, stress-strain and electrochemical measurements.

CHAPTER 3. STRUCTURE AND PROPERTIES OF Ni-Ti-BASED RAPIDLY SHAPE MEMORY ALLOYS

3.1. Structure and properties of Ni-Ti-Cu rapidly quenched alloy

Studies have shown that adding Cu to Ni-Ti alloy can reduce temperature hysteresis and increase the mechanical properties of the alloy. Therefore, we studied the structure and properties of $Ni_{50-x}Ti_{50}Cu_x$ alloy ribbons (x = 0, 5, 10, 15 and 20).

To check whether the elemental ratio in the sample after fabrication has decreased or not, we used the EDX method. The analysis results showed that the change rule of the atomic percentage of the elements determined by EDX spectroscopies is almost consistent with the atomic composition of the initial nominal composition.

XRD patterns of the $Ni_{50-x}Ti_{50}Cu_x$ (x = 0, 5, 10, 15 và 20) ribbons are shown in Figure 3.4a. One can realize that all the samples contain a single crystalline phase of (Ni,Cu)Ti at room temperature corresponding to the B19' (orthorhombic)-martensitic structure. It is seen that the diffraction peak shifts to lower 2θ with increasing Cu content.

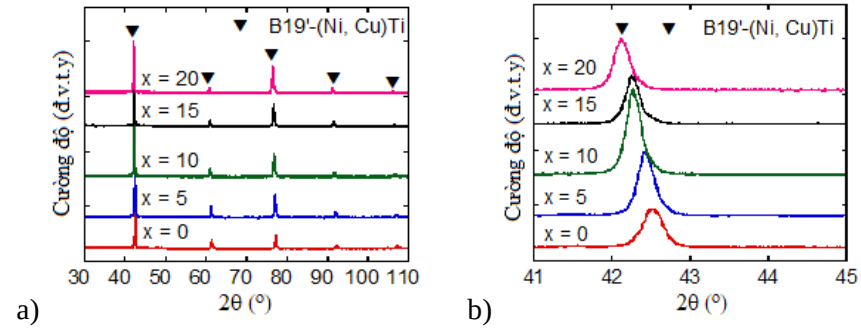

Figure 3.4. XRD patterns of the $Ni_{50-x}Ti_{50}Cu_x$ (x = 0, 5, 10, 15 and 20) alloy ribbons (a) and an enlarged part at 2θ in the range of 41-45° (b).

The DSC curves in the heating mode of the $Ni_{50-x}Ti_{50}Cu_x$ alloy ribbons with x = 0 and 15 are shown in Figure 4. The structural transition temperatures of the $Ni_{50-x}Ti_{50}Cu_x$ alloy ribbons with x = 0 and 15 are all less than 100°C. Figure 3.9 shows the Vickers hardness values with increasing Cu concentration of the Ni-Ti-Cu alloy ribbons. It is clear that the addition of Cu slightly reduces the hardness of the Ni-Ti alloy ribbons from 398 HV (for x = 0) to 318 HV (for x = 20).

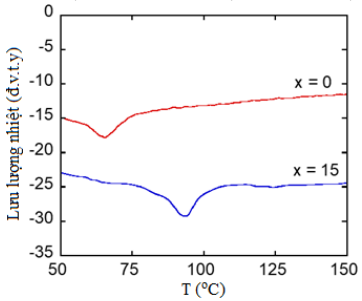

Figure 3.8. DSC curves in heating mode of SMA $Ni_{50-x}Ti_{50}Cu_x$ with x = 0 and 15.

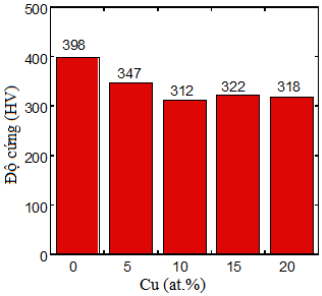

Figure 3.9. Vickers Hardness (HV) of SMA $Ni_{50-x}Ti_{50}Cu_x$ (x = 0, 5, 10, 15 and 20).

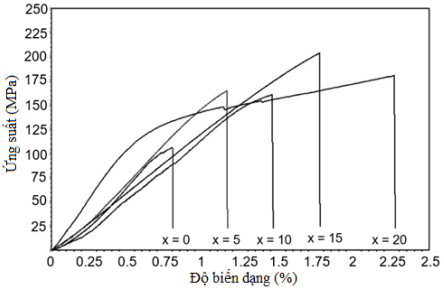

Figure 3.10. Stress-strain curvers of $Ni_{50-x}Ti_{50}Cu_x$ (x = 0, 5, 10, 15 and 20) ribbons.

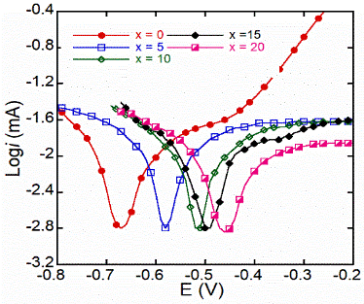

Figure 3.12. Potentiodynamic polarization curves of $Ni_{50-x}Ti_{50}Cu_x$ (x = 0, 5, 10,15 and 20) alloy ribbons.

Figure 3.10 shows the stress-strain curves of the $Ni_{50-x}Ti_{50}Cu_x$ alloy ribbons at room temperature. The tensile strength of the $Ni_{35}Ti_{50}Cu_{15}$ alloy ribbons can be up to 203.9 MPa, which is about 88% higher than that of the

$Ni_{50}Ti_{50}$ alloy ribbons. The tensile strain and elastic modulus increase from 0.8 to 2.27% and 5.64 to 29.17 GPa when the Cu concentration increases from 0 to 20 at.%.

The anodic polarization curve of the $Ni_{50-x}Ti_{50}Cu_x$ alloy ribbons (x = 0, 5, 10, 15 and 20) is shown in Figure 3.12. The CR of the $Ni_{50}Ti_{50}$ alloy ribbons obtained was 0.27×10^{-2} mm/year while that of the $Ni_{45}Ti_{50}Cu_5$ alloy ribbons was 1.82×10^{-2} mm/year. Therefore, the substitution of Cu for Ni reduced the corrosion resistance of the alloy. However, this decrease was so small that it did not significantly affect the application of the alloy.

3.2. Structure and properties of Ni-Cu-Ti-Zr-A (A = Hf, Nb, Co, Cr and Ga) rapidly quenched high entropy shape memory alloy

To improve the application of this alloy, we add more elements to the Ni-Ti alloy to make HESMA. The $Ni_{25}Cu_{25}Ti_{16.667}Zr_{16.667}A_{16.667}$ (A = Hf, Nb, Co, Cr and Ga) alloy ribbons are denoted according to table 3.6.

Table 3.6. Symbols and percentage of the molar concentration of the elements in the $Ni_{25}Cu_{25}Ti_{16.667}Zr_{16.667}A_{16.667}$ (A = Hf, Nb, Co, Cr and Ga) alloy ribbons.

Symbol	Ni (at.%)	Cu (at.%)	Ti (at.%)	Zr (at.%)	A (at.%)
S1	50	0	50	0	0
S2	25	25	50/3	50/3	50/3 (Hf)
S3	25	25	50/3	50/3	50/3 (Nb)
S4	25	25	50/3	50/3	50/3(Co)
S5	25	25	50/3	50/3	50/3(Cr)
S6	25	25	50/3	50/3	50/3 (Ga)

Figure 3.14 is the surface SEM image of S1, S2, S4 and S5 alloy ribbons. For S1 alloy ribbons, we can observe clear grain boundaries. Meanwhile, we cannot observe grain boundaries in S2 and S4 alloy ribbons. S5 alloy ribbon has relatively blurry, not sharp grain boundaries.

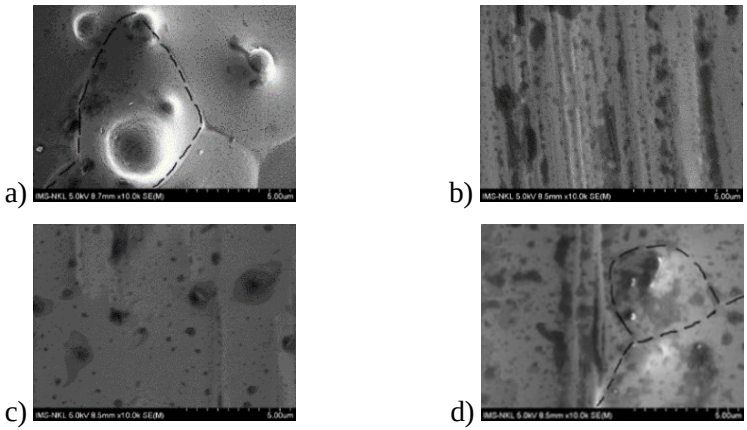

Figure 3.14. SEM images of S1 (a), S2 (b), S4 (c) and S5 (d). (The dashed lines in the figure are for easy visualization of the crystal grains).

The DTA curves of S1, S3, S4 and S5 alloy ribbons are shown in figure 3.16. The structural transformation temperature of S3, S4 and S5 alloy ribbons occurs in the range of 500-650ºC.

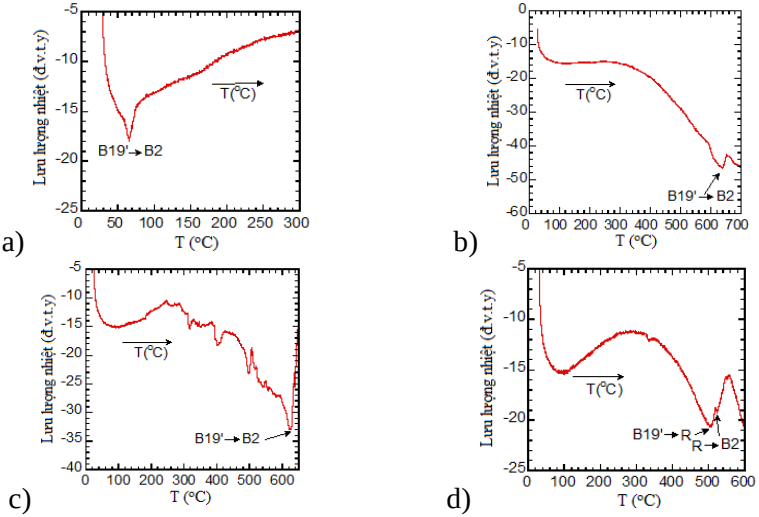

Figure 3.16. DTA curve of S1 (a), S3 (b), S4 (c) and S5 (d) alloy ribbons.

The stress-strain curves of the alloy ribbons indicate that the S2, S3 and S4 alloy ribbons have higher tensile strength and elastic modulus than the S1 sample. The tensile strength and elastic modulus of the S1, S2, S3 and

S4 alloy ribbons is arranged in the following order S1 < S3 < S4 < S2. However, the deformation of the sample increases slightly.

Figure 3.22 shows the corrosion rates of the S2, S3, S4, S5 and S6 alloy ribbons. The S6 alloy ribbons have the lowest corrosion rate of 0.09 x 10^{-2} mm/year while the S5 alloy ribbons have the highest corrosion rate of 0.29 x 10^{-2} mm/year.

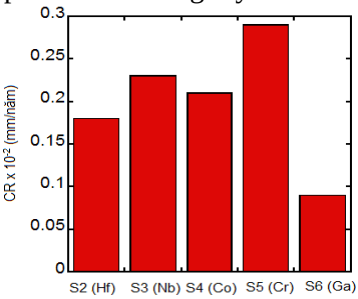

Figure 3.22. Corrosion rate (CR) of S2, S3, S4, S5 and S6 alloy ribbons.

Chapter 4. STRUCTURE AND PROPERTIES OF Ni-Mn BASED SHAPE MEMORY ALLOYS

4.1. Structure and properties of (Ni,Co)-Mn-Ga rapidly quenched alloy ribbons

4.1.1. Structure and properties of $Ni_{50}Mn_{50-x}Ga_x$ (x = 17 - 21) alloy ribbons

Ni-Mn-Ga alloys have large deformation induced by magnetic fields and are being studied a lot. However, there are still some aspects that have not been clarified, so we conducted a study on the structure and properties of the $Ni_{50}Mn_{50-x}Ga_x$ (x = 17 - 21) alloy ribbons.

The XRD patterns of the alloy strips obtained at room temperature are shown in Figure 4.1. With increasing Ga-concentration, the $L2_1$ austenitic structure phase gradually decreases, while the 5 M and 7 M martensitic structural phases increase.

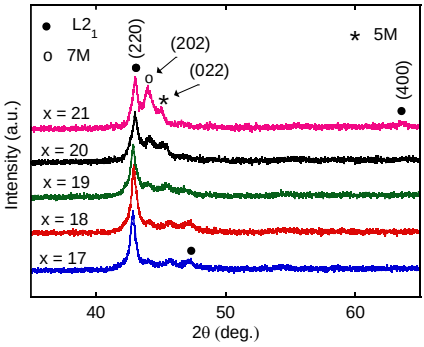

Figure 4.1. XRD patterns of $Ni_{50}Mn_{50-x}Ga_x$ (x = 17, 18, 19, 20 and 21)

From figure 4.2, it can be seen that except for sample x = 17, all samples have martensitic-austenitic (M-A) structural transformation. When the magnetic field reaches 12 kOe, the M-A structural transformation is almost not observed in all samples (figure 4.2c).

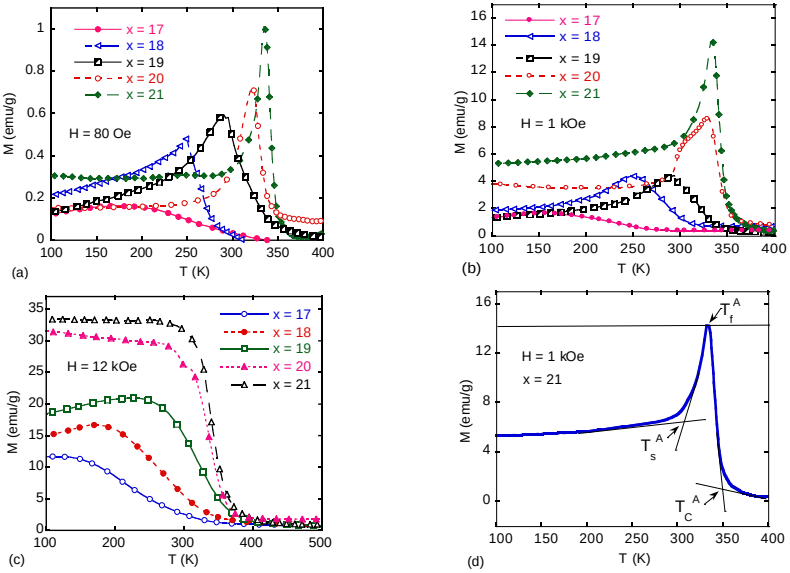

Figure 4.2. Thermomagnetisation curves of $Ni_{50}Mn_{50-x}Ga_x$ (x = 17 - 21) alloy ribbons in an applied magnetic field of 80 Oe (a), 1 kOe (b) and 10 kOe (c) and describe how to determine structural transition temperatures (d).

To clearly see the effect of magnetic field on the structural transformation of the alloy ribbons, the M(T) curves were measured in the magnetic field from 0.1-10 kOe with Ga concentration of 20 at.% (figure 4.3). The M-A structural transformation appeared clearly in the magnetic field range from 0.1 to 6 kOe.

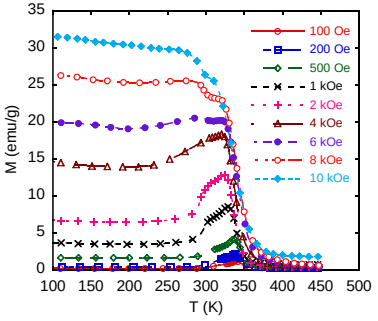

Figure 4.3. M(T) curves of $Ni_{50}Mn_{30}Ga_{20}$ alloy ribbons in various magnetic fields in the range of 0.1-10 kOe.

4.1.2. Structure and properties of $Ni_{50-x}Co_xMn_{29}Ga_{21}$ (x = 0, 2, 4, 6, 8) alloy ribbons

Previous research results showed that $Ni_{50}Mn_{29}Ga_2$ MSMA has a clear martensitic-austenitic structural transformation or SME. The substitution of Co for Ni in Ni-Mn-Ga alloy has created changes in the structure and magnetic properties of the alloy. Therefore, we continued to study the influence of Co on the structure and magnetic properties of $Ni_{50-x}Co_xMn_{29}Ga_{21}$ (x = 0, 2, 4, 6 and 8) MSMA fabricated by using melt-spinning method.

Similar to other samples, we also checked whether the alloy composition after melting is guaranteed. Because Mn is easily evaporated during the melting process. The results showed that the atomic percentage of the elements determined by EDX spectroscopy is almost consistent with the atomic composition of the initial nominal composition.

The XRD pattern of the $Ni_{50-x}Co_xMn_{29}Ga_{21}$ (x = 0, 2, 4, 6 and 8) alloy ribbons is shown in figure 4.5. As the Co concentration increases, the austenitic phase corresponding to the cubic Ni_2MnGa structure increases, while the martensitic phase with the tetragonal Ni_2MnGa structure gradually decreases.

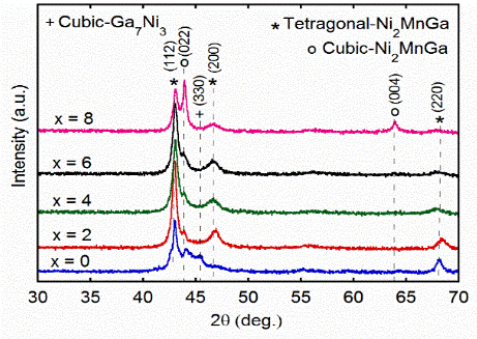

Figure 4.5. XRD patterns of the $Ni_{50-x}Co_xMn_{29}Ga_{21}$ (x = 0, 2, 4, 6 and 8) ribbons.

Figure 4.6 shows SEM images of the $Ni_{50-x}Co_xMn_{29}Ga_{21}$ (x = 0, 2, 4, 6 và 8). All the samples have good directional crystallization. The crystalline grains in rod-like shapes are almost parallel to each other and perpendicular to the surface of the ribbon. It can be noted that the directional crystallization of the grains decreases with increasing Co-concentration.

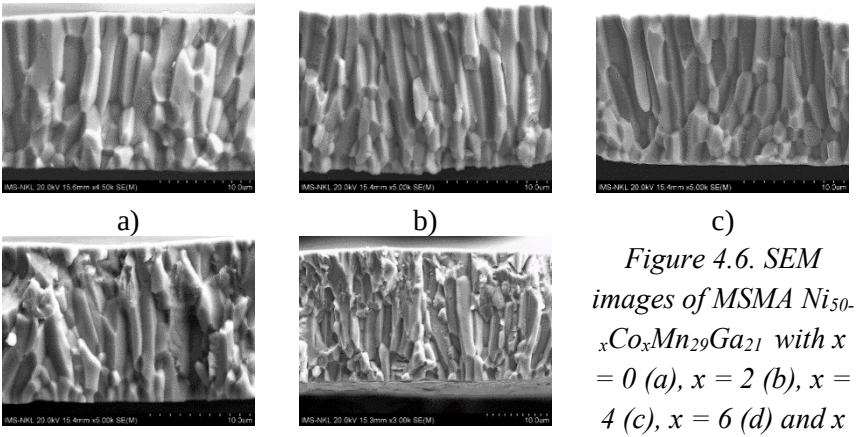

a) b) c)

d) e)

Figure 4.6. SEM images of MSMA $Ni_{50-x}Co_xMn_{29}Ga_{21}$ with x = 0 (a), x = 2 (b), x = 4 (c), x = 6 (d) and x = 8 (e).

The M(T) curves of the $Ni_{50-x}Co_xMn_{29}Ga_{21}$ (x = 0, 2, 4, 6 and 8) alloy ribbons in a magnetic field of 1 kOe are shown in fig 4.8. The M-A structural transformation appears with increasing Co concentration from 0 to 6 at.%.

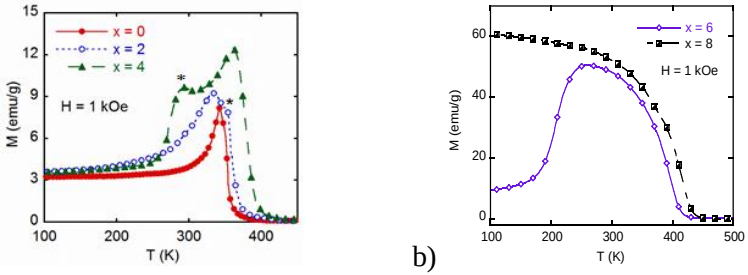

a) b)

Figrure 4.8. M(T) curves of the $Ni_{50-x}Co_xMn_{29}Ga_{21}$ alloy ribbons with x = 0, 2, 4 (a) and x = 6, 8 (b) in an applied magnetic field of 1 kOe.

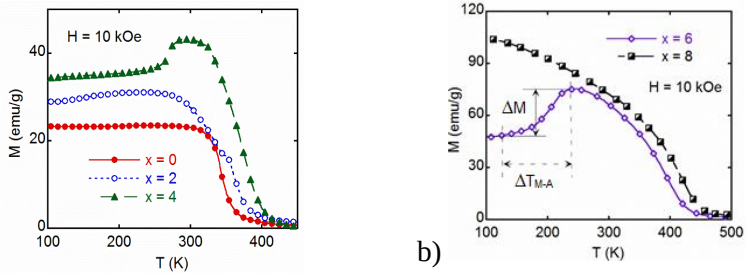

a) b)

Figure 4.9. M(T) curves of the $Ni_{50-x}Co_xMn_{29}Ga_{21}$ alloy ribbons with x = 0, 2, 4 (a) and x = 6, 8 (b) in an applied magnetic field of 10 kOe.

In addition, for the samples with Co concentrations of 2 and 4 at.%, the M-A structural transformation was not observed on the M(T) curve measured in a magnetic field of H = 10 kOe (figure 4.9). Thus, the M-A structural transformation depends on both temperature and magnetic field.

Figure 4.11 is the DSC curve of $Ni_{50-x}Co_xMn_{29}Ga_{21}$ MSMA (x = 0, 2 and 4) during heating and cooling processes. The T_s^A, T_f^A, T_s^M, T_f^M structural transformation temperatures increase with increasing Co concentration. The thermal hysteresis ($\Delta T = T_{M-A} - T_{A-M}$) increases from 13 to 16 K when the Co concentration increases from 0 to 4 at.%.

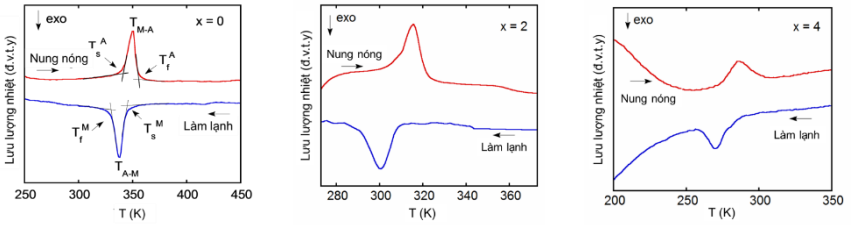

Figure 4.11. Heating and cooling DSC curves of the $Ni_{50-x}Co_xMn_{29}Ga_{21}$ (x = 0, 2, and 4) alloy ribbons.

4.2. Structure and properties of Ni-Co-Mn-Al rapidly quenched alloy ribbons

4.2.1. Structure and properties of $Ni_{50-x}Co_xMn_{50-y}Al_y$ (x = 5 - 9 và y = 18, 19) alloy ribbons

Studies have shown that Ni-Mn-Al MSMAs have better mechanical properties than the relatively brittle Ni-Mn-Ga MSMAs. Therefore, Ni-Mn-Al alloys become good candidates for applications as shape memory materials. Previous studies have shown that at Al concentrations in the range of 18-19%, the alloy can exhibit M-A structural transformation or shape memory effect. Therefore, in this section, we systematically study the structure and properties of $Ni_{50-x}Co_xMn_{50-y}Al_y$ alloy ribbons (x = 5 - 9 and y = 18, 19).

XRD patterns of MSMA $Ni_{50-x}Co_xMn_{50-y}Al_y$ are shown in Figure 4.13. For ribbons with Al concentration of 18 at%, the fraction of the NiMn crystalline phase gradually decreases as the Co concentration is increased,

meanwhile, the fraction of the Ni_2MnAl phase is increased. For alloy ribbons with Al concentrations of 19 at%, the fraction of these crystalline phases does not change much with different Co concentrations except for a small increase of the NiMn phase in the sample with Co concentration of 5 at.%.

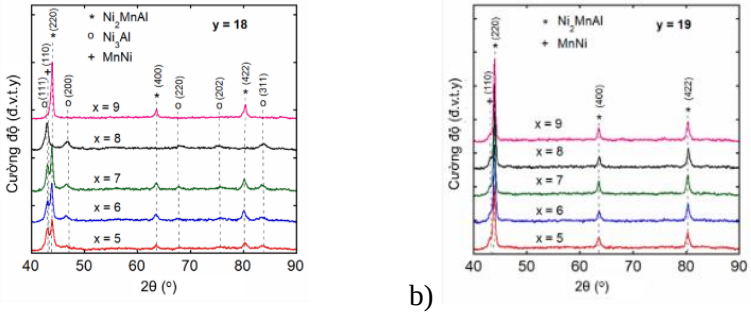

Figure 4.13. XRD patterns of MSMA $Ni_{50-x}Co_xMn_{50-y}Al_y$ with: y = 18 (a) and y = 19 (b).

The M(T) curves with Al concentration of 18 at.% in applied magnetic fields of 100 Oe and 10 kOe are shown in figures 4.16. The M-A structural transformation is observed on all the ribbon samples with Co concentration from 5 to 8 at%. Notably, the sample with Co concentration of 15 at.% was observed only at a magnetic field of 10 kOe.

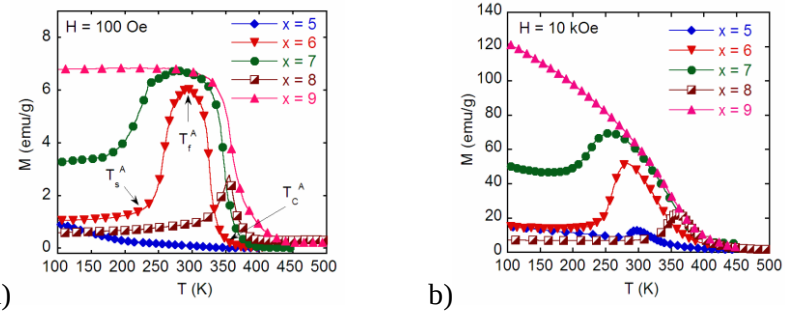

Figure 4.16. The M(T) curves of the $Ni_{50-x}Co_xMn_{50-y}Al_y$ ribbons with y = 18 in the magnetic field of: 0.1 kOe (a) and 10 kOe (b).

To see more clearly the magnetic field dependence of the M-A structural transformation, the M(T) curves with a Co concentration of 5 at.% were measured at different external magnetic fields (figure 4.18). The M-A

structural transformation occurs only when the external magnetic field is greater than 500 Oe.

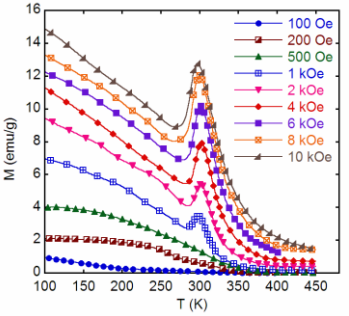

Figure 4.18. M(T) curve of MSMA $Ni_{50-x}Co_xMn_{50-y}Al_y$ with x = 5, y = 18 in different magnetic fields.

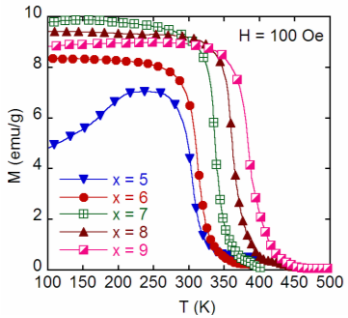

Figure 4.17. The M(T) curves of the $Ni_{50-x}Co_xMn_{50-y}Al_y$ ribbons with y = 19 in magnetic field of: 0.1 kOe.

For the ribbon samples with Al concentration of 19 at.%, the M-A phase transformation is only observed when the Co concentration is 5 at% (figure 4.17).

4.2.2. Structure and properties of $Ni_{50-x}Co_xMn_{50-y}Al_y$ (x = 5 - 10 và y = 16, 17) alloy ribbons

With the studied concentration range of Co (x = 5 - 10) and Al (y = 18 - 19), the M-A structural transformation temperatures of all alloy ribbons are lower than room temperature (T_{room}). For SMAs, many practical applications require the temperature of the M-A structural transformation temperatures to be higher than T_{room} and the width of the transformation is sufficiently small. Therefore, we continue to study the $Ni_{50-x}Co_xMn_{50-y}Al_y$ alloy ribbons with x = 5 - 10 and y = 16 - 17.

The SEM image of the cross-section of MSMA $Ni_{50-x}Co_xMn_{50-y}Al_y$ with y = 17 is shown in Figure 4.21. As the Co concentration increases, the austenitic phase fraction increases, leading to the formation of grains with larger widths. The predominance of the austenitic phase is also demonstrated through M(T) measurements.

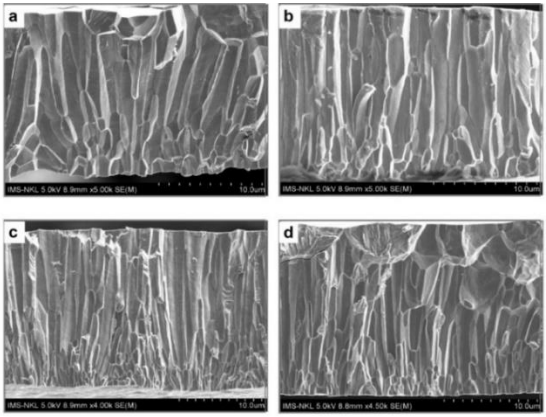

Figure 4.21. SEM images of $Ni_{50-x}Co_xMn_{50-y}Al_y$ MSMA with y = 17 and x varying: x = 5 (a), x = 6 (b), x = 7 (c), x = 8 (d).

The M(T) curves of MSMA $Ni_{50-x}Co_xMn_{50-y}Al_y$ in different applied magnetic fields of 100 Oe and 10 kOe are shown in figures 4.23 and 4.28. For Al concentration of 17 at.%, all the samples, except the sample with x = 9, reveal a clear martensitic-austenitic (M- A) structural transformation. Besides temperature, the external magnetic field also affects the M- A structural transformation of the alloy ribbons.

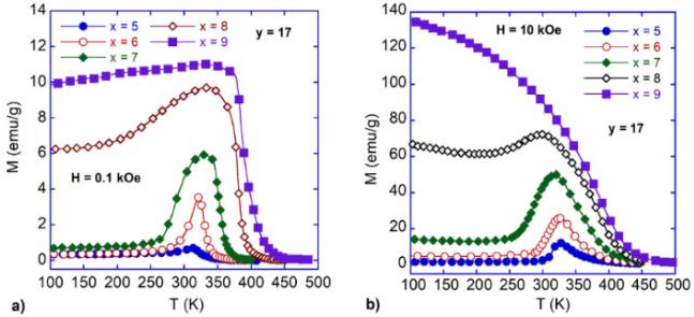

Hình 4.23. M(T) curves of the $Ni_{50-x}Co_xMn_{50-y}Al_y$ ribbons with x = 5-9 and y = 17 in magnetic fields of: 0.1 kOe (a) and 10 kOe (b).

For the ribbon samples with Al concentration of 16 at.%, all the samples, except the one with x = 7, undergo a structural transformation process from martensite to austenite. Notably, while T_C^A tends to increase with Co concentration, T_s^A and T_f^A vary irregularly.

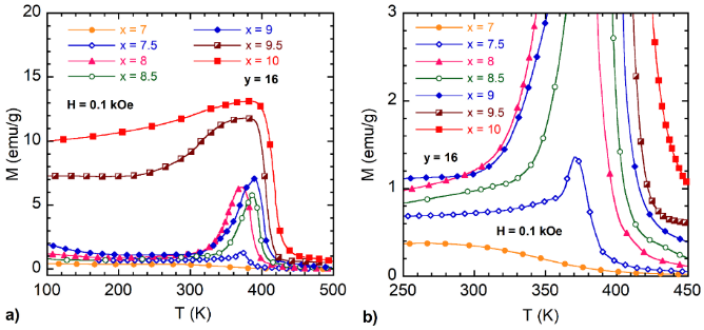

Figure 4.28. M(T) curves of MSMA $Ni_{50-x}Co_xMn_{50-y}Al_y$ with (x = 7 - 10 and y = 16) in magnetic fields of 0.1 kOe (a) and their enlarged region around phase transformation temperatures (b).

4.2.3. Structure and properties of $Ni_{50-x}Co_xMn_{50-y}Al_y$ (x = 7 - 13, y = 15)alloy ribbons

With Al concentrations in the range of 16 - 19 at.%, it is shown that the M-A structural transformation tends to shift to higher temperatures with decreasing concentration of Al and the lower the concentration of Al, the higher the critical concentration of Co. Therefore, in this study, we further reduced the Al concentration and investigated the structure and properties of $Ni_{50-x}Co_xMn_{35}Al_{15}$ (x = 7 - 13) alloy ribbons.

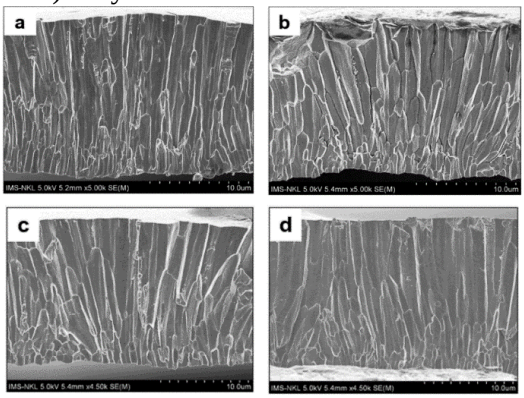

Figure 4.32. SEM images of MSMA $Ni_{50-x}Co_xMn_{35}Al_{15}$: x = 8 (a), x = 9 (b), x = 10 (c) and x = 11 (d).

SEM images of the cross sections of typical alloy ribbons (x = 8, 9, 10 and 11) are shown in figure 4.32. It can be seen that all the alloy ribbons have

highly oriented crystallization of rod-shaped grains perpendicular to the ribbon surface.

Figure 4.34 shows elemental mapping images for a typical sample with x = 11. One can see that all the elements of Al, Mn, Co and Ni are almost evenly distributed in the alloy ribbon.

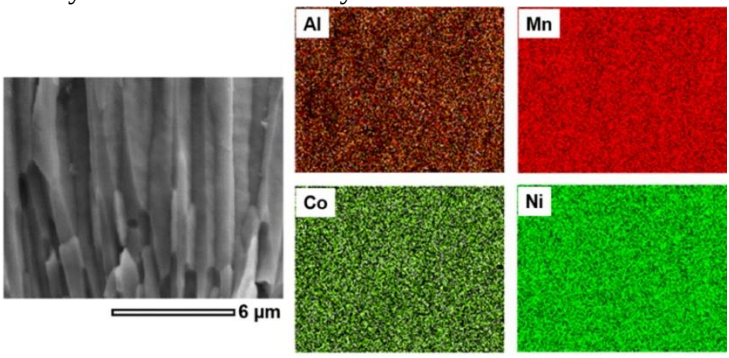

Figure 4.34. Elemental mapping images of $Ni_{39}Co_{11}Mn_{35}Al_{15}$ ribbon (x = 11).

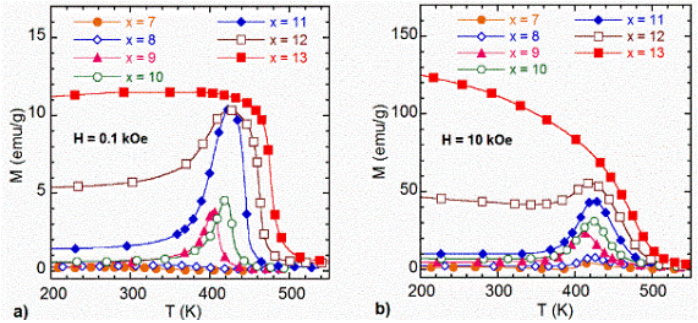

Figure 4.35. M(T) curves of $Ni_{50-x}Co_xMn_{35}Al_{15}$ ribbons in magnetic field of 0.1 kOe (a) and 10 kOe (b).

The M(T) curves of the $Ni_{50-x}Co_xMn_{35}Al_{15}$ (x = 7 - 13) alloy ribbons measured in various magnetic field of 0.1 and 10 kOe are presented in figure 4.35. It can be seen that the M-A structural transformation is observed in the samples with the Co concentrations in the range of 7 to 12 at%. Notably, in the samples with the Co concentrations of 7 and 8 at%, the M-A phase transformation is only observed on the M(T) curves measured in the high

external magnetic field of 10 kOe. It is noteworthy that the M-A structural transformation process occurs entirely above room temperature, in the range of 360 - 430 K for Co concentrations from 7 to12 at.%.

The mechanical properties of the $Ni_{50-x}Co_xMn_{35}Al_{15}$ (x = 7-11) alloy ribbons were characterized by tensile stress-strain measurements (figure 4.39). When the Co concentration increases from 7 to 11 at%, the tensile strength increases from 11.6 MPa to 22.3 MPa, while the tensile strain of the alloy decreases from 3.8 to 2.3%.

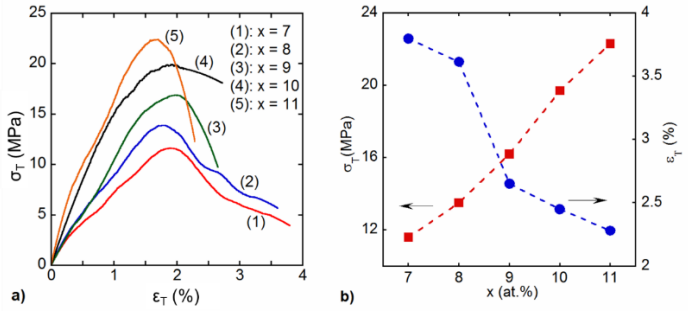

Figure 4.39. Stress-strain curves (a) and Co concentration dependence of tensile strength and tensile strain (b) of $Ni_{50-x}Co_xMn_{35}Al_{15}$ (x = 7-11) ribbons.

The corrosion resistance (CR) of the alloy was investigated on typical samples (x = 7, 10 and 13). The CR were 0.82×10^{-2}, 0.93×10^{-2} and 0.85×10^{-2} mm/year corresponding to the Co concentrations of 7, 10 and 13 at%, respectively. Compared with the CR of the Ni-Ti and Ni-Ti-Cu shape memory alloy ribbons fabricated and measured under the same conditions, the CR of the Ni-Co-Mn-Al alloy has the same order of magnitude.

CONCLUSION

1. Researched technology and successfully manufactured Ni-Ti and Ni-Mn-based shape memory alloy (SMA) by using a melt-spinning method.

+ $Ni_{50-x}Ti_{50}Cu_x$ (x = 0 - 20)
+ $Ni_{25}Cu_{25}Ti_{16.667}Zr_{16.667}A_{16.667}$ (A = Hf, Nb, Co, Cr and Ga)
+ $Ni_{50}Mn_{50-x}Ga_x$ (x = 17 - 21)
+ $Ni_{50-x}Co_xMn_{29}Ga_{21}$ (x = 0 - 8)

+ $Ni_{50-x}Co_xMn_{50-y}Al_y$ (x = 5 - 13; y = 15 - 19)

2. Investigated structure and properties of the Ni-Ti-based shape memory alloys:

- The Ni-Ti alloys all exhibit a martensitic (B19')-austenitic (B2) structural transformation related to the shape memory effect (SME). In addition, the B19'-R-B2 intermediate transformation is observed on the Cr-containing alloys.

- The structural transformation temperature, tensile strain and tensile strength increase, while the hardness and corrosion resistance decrease when the Cu concentration is increased from 0 to 20 at.%. $Ni_{30}Ti_{50}Cu_{20}$ SMAs has the best mechanical properties with a tensile strain and tensile strength of ~2.3% and ~180 MPa, respectively.

- The addition of Cu, Zr, Hf, Nb, Co, Cr and Ga elements to the Ni-Ti alloys enhance the structural transformation temperature above 500°C. The Hf-containing alloy ribbons have the highest tensile strength and tensile strain of ~669 MPa and ~0.9%, respectively. Although the $Ni_{25}Cu_{25}Ti_{16,667}Zr_{16,667}A_{16,667}$ high entropy shape memory alloys (HESMAs) have lower strain than the $Ni_{50-x}Ti_{50}Cu_x$ SMAs, they have superior hardness and corrosion resistance.

3. Investigated structure and properties of the Ni-Mn-based shape memory alloys:

- Most of the obtained samples have (B19', 5M, 7M, $L1_0$) martensitic - (B2, $L2_1$) austenitic structural transformation related to SME.

- Some samples show good orientational crystallization which is beneficial for the application.

- All samples show soft magnetic with small coercivity (H_c < 100 Oe).

- The structural phase transition temperature shifts towards lower temperature as the magnetic field increases.

- The structural phase transition temperature and magnetic phase transition can be adjusted as desired by changing the appropriate concentrations of Co, Ga and Al.

- With the $Ni_{50}Mn_{50-x}Ga_x$ alloy system, the martensitic start temperature (T_s^M), martensitic finish temperature (T_f^M) and Curie

temperature of austenitic phase (T_C^A) of the alloy increase with increasing Ga concentration. When adding Co, T_s^M and T_f^M of $Ni_{50-x}Co_xMn_{29}Ga_{21}$ alloy decrease, while T_C^A increase. The martensitic-austenitic structural transformation temperature of $Ni_{50-x}Co_xMn_{29}Ga_{21}$ alloy appeared in the temperature range from 180 to 340ºC.

- With $Ni_{50-x}Co_xMn_{50-y}Al_y$ alloy system, T_s^A decreased while T_f^A and T_C^A increased when increasing Co concentration and decreasing Al concentration. The martensitic-austenitic structural transformation temperature was in the range from 150 to 430ºC.

From the obtained research results, we see the need to continue researching in the following directions:

- Research to increase the recovery strain of Ni-Ti-based high entropy shape memory alloys.

- Research to increase the good mechanical properties of Ni-Mn-based magnetic shape memory alloys.

LIST OF REPORTED PUBLICATIONS

1. Nguyen Huy Dan, Kieu Xuan Hau, Nguyen Hai Yen, Pham Thi Thanh, Nguyen Huy Ngoc, Truong Viet Anh, Nguyen Thi Nguyet Nga, Do Thi Kim Anh, 2022, Structure and magnetic properties of $Ni_{50-x}Co_xMn_{50-y}Al_y$ (x = 5 - 9, y = 18 - 19) shape memory alloy ribbons, *Journal of Alloys and Compounds*, 916, pp. 165470.
2. Kieu Xuan Hau, Nguyen Hai Yen, Nguyen Huy Ngoc, Truong Viet Anh, Pham Thi Thanh, Nguyen Van Toan and Nguyen Huy Dan, 2023, Influence of Cu concentration on structure, mechanical properties and corrosion resistance of TiNiCu shape memory Alloy ribbons, *Materials Transactions*, 64, pp. 849- 854.
3. Nguyen Hai Yen, Kieu Xuan Hau, Nguyen Huy Ngoc, Pham Thi Thanh, Truong Viet Anh and Nguyen Huy Dan, 2023, Influence of Co on structure and magnetic properties of $Ni_{50-x}Co_xMn_{29}Ga_{21}$ shape memory alloy ribbons, *Materials Transactions*, 64 pp. 2560-2567.
4. Nguyen Huy Dan, Kieu Xuan Hau, Nguyen Hai Yen, Pham Thi Thanh, Nguyen Huy Ngoc, Truong Viet Anh, 2024, Highly oriented crystallization, and tunable structural transformation and magnetic

transition in Ni-Co-Mn-Al shape memory alloys, *Journal of Magnetism and Magnetic Materials*, 589, pp. 171576.

5. Hai Yen Nguyen, Xuan Hau Kieu, Huy Ngoc Nguyen, Thi Thanh Pham, Tran Dang Thanh, Quang Nhat Le and Huy Dan Nguyen, 2022, Structure and magnetic properties of Ni-Mn-Ga shape memory alloys, *Advances in Natural Sciences: Nanoscience and Nanotechnology*, 13, pp. 015014.
6. Nguyen Huy Dan, Kieu Xuan Hau, Nguyen Hai Yen, Pham Thi Thanh, Nguyen Huy Ngoc, Dang Doan Nuoi, Tran Dang Thanh, 2021, Investigation of shape memory effect in Ni-Ti based alloys, *Communications in Physics*, 31, pp. 343-352.
7. Kieu Xuan Hau, Nguyen Hai Yen, Nguyen Huy Ngoc, Truong Viet Anh, Pham Thi Thanh, Nguyen Van Toan, Tran Dang Thanh, Nguyen Huy Dan, 2022, Investigation of structure and properties of melt-spun NiTi based shape memory alloys, *Vietnam Journal of Science and Technology*, 60, pp. 1023-1031.
8. Kieu Xuan Hau, Nguyen Hai Yen, Nguyen Huy Ngoc, Truong Viet Anh, Pham Thi Thanh, Nguyen Huy Dan, 2021, Influence of Cu on structure and properties of Ti-Ni-Cu shape memory alloys, *The 10th International Workshop on Advanced Materials Science and Nanotechnology (IWAMSN)*, pp. 203-208.
9. Nguyen Huy Dan, Kieu Xuan Hau, Nguyen Hai Yen., Nguyen Huy Ngoc, Truong Viet Anh, Pham Thi Thanh, Nguyen Thi Nguyet Nga, Do Thi Kim Anh, 2021, Tuning structural transformation and magnetic transition in Ni-Co-Mn-Al shape memory alloy, *The 10th International Workshop on Advanced Materials Science and Nanotechnology (IWAMSN)*, pp. 214-218.
10. Kiều Xuân Hâu, Nguyễn Hải Yến, Phạm Thị Thanh, Nguyễn Văn Toàn, Nguyễn Huy Ngọc, Trương Việt Anh, Đinh Chí Linh, Nguyễn Huy Dân, 2023, Nghiên cứu cấu trúc, tính chất từ và cơ của các băng hợp kim nhớ hình $Ni_{50-x}Co_xMn_{50-y}Al_y$ (x = 7 - 13, y = 15), *Hội nghị Vật lý Chất rắn và Khoa học Vật liệu Toàn quốc (SPMS)*, pp. 76-81.